Available online at www.eccomasproceedia.org
Eccomas Proceedia COMPDYN (2023) 759-769

ECCOMAS
Proceedia

COMPDYN 2023
9th ECCOMAS Thematic Conference on
Computational Methods in Structural Dynamics and Earthquake Engineering
M. Papadrakakis, M. Fragiadakis (eds.)
Athens, Greece, 12-14 June 2023

EFFECT OF THE SLAB ON THE INELASTIC RESPONSE OF REINFORCED CONCRETE BEAM-COLUMN JOINTS: A NUMERICAL INVESTIGATION

Charoula D. Zaki[1] **and Vassilis K. Papanikolaou**[2]

[1] REDI Engineering Solutions
e-mail: charoulaz@civil.auth.gr

[2] Aristotle University of Thessaloniki
School of Civil Engineering
billy@civil.auth.gr

Abstract

This paper presents a numerical investigation into the effect of the slab presence on the inelastic response of reinforced concrete beam-column joints, which is usually ignored in experimental practice due to cost and implementation challenges. The study examines different joint types, including corner, exterior, and interior joints, designed according to Eurocodes 2 and 8. The beam-column joints are analyzed in three levels, based on their configuration: (i) simple planar beam-column joint, (ii) addition of a transverse beam, and (iii) complete model including the slab. Three-dimensional nonlinear finite element analysis is employed to model the beam-column joints using solid elements for concrete and embedded linear elements for reinforcement bars. The analysis comprises two successive loading types: axial compressive load and lateral monotonic seismic load as prescribed displacement. The numerical results include comparative analyses of the three levels based on response (pushover) curves, as well as observations on cracks, yielding of reinforcement bars, and failure mechanisms.

Keywords: Reinforced concrete, beam-column joint, slab, inelastic response, finite element analysis, Eurocodes, seismic loading.

ISSN:2623-3347
Peer-review under responsibility of the organizing committee of COMPDYN 2023.
doi: 10.7712/120123.10433.22212

1 INTRODUCTION

Beam-column joints are key structural components in reinforced concrete (R/C) moment-resisting frame structures and dual systems. Inadequately reinforced joints against earthquake-induced lateral forces can pose substantial risks of premature local failure, leading to partial or even global collapse. This risk is particularly pronounced in older buildings, which often lack compliance with current codes and contain poorly detailed beam-column joints, making them more susceptible to severe seismic consequences. At the same time, a common practice in many relevant experimental studies, often driven by cost and implementation challenges, is the exclusion of the transverse beam and slab presence in the analysis of the inelastic response of reinforced concrete beam-column joints. The slab and the transverse beam are integral components that can contribute to joint flexural strength and ductility. By ignoring these elements, experimental studies may not adequately capture the expected behavior of beam-column joints under various load conditions.

The above simplification could also lead to an inaccurate calculation of the beam flexural resistance moment, a critical parameter in the context of capacity design. Capacity design is a design philosophy that ensures that inelastic deformation occurs at specified locations within the structure, while other areas remain essentially elastic, even during extreme events such as earthquakes. If the contribution of the slab and the transverse beam to the resistance moment is overlooked, the capacity design could be deficient, possibly leading to an unfavorable strong beam / weak column connection. To implicitly address this issue, modern building codes [1] often incorporate overstrength factors and slab effective lengths in their design guidelines. However, it is still important for numerical procedures to consider the presence of the slab and the transverse beam to ensure accurate resistance moment calculations and a more reliable capacity design.

A few experimental studies have investigated the influence of the transverse beam and slab on beam-column joint configurations. For instance, Kam et al. [2] examined the performance of exterior R/C beam-column joints, representative of pre-1970s construction practices, both with and without the slab. The beam-column joint subassemblies were subjected to uni- and bi-directional static lateral loading with varying axial loading. Comparisons between global and local behavior of the specimens highlighted the influential role of the slab and the transverse beam in contributing to the resistance mechanism of the beam-column-joint subassembly. In contrast to the limited experimental studies, various numerical studies have employed three-dimensional nonlinear finite element analyses on beam-column joints exposed to seismic loading. Allam et al. [3] conducted a study on a planar corner R/C beam-column joint, without slab and transverse beam, under monotonic loading. The study showed that the beam ultimate load significantly increased as the concrete strength, axial load and joint reinforcement increased. Tambusay et al. [4] tested interior, corner and exterior joint configurations by adjusting the boundary conditions. The joints were subjected to reversed cyclic loading, capturing the cyclic hysteretic response, progressive degradation of strength and stiffness, cracking, and failure mode. A more elaborate approach taken by Santarsiero and Masi [5] used numerical analyses on the exterior R/C joint, based on previous experimental test results, to evaluate the influence of the transverse beam and slab under monotonic loading. Numerical results showed that the tension flange effect of slab can significantly increase negative moment in beams framing into beam-column joints. In a similar study, Mou et al. [6] examined the seismic performance of a composite concrete-steel beam-column joint configuration, both with and without an overlying concrete slab.

It is evident that the analysis of transverse beam and slab interactions has received only recent attention and requires further examination. In line with this goal, the present study aims

to further illustrate the inelastic behavior of various reinforced concrete (R/C) beam-column joint configurations, considering the influence of transverse beam and slab additions.

2 NUMERICAL MODELING AND ANALYSIS

To select a realistic and representative set of different beam-column joint configurations typically found in reinforced concrete (R/C) buildings, while ensuring their design compatibility with Codes of practice, subassemblies were directly extracted from a typical symmetrical R/C building, already designed and detailed according to Eurocodes 2 (EN1992-1-1) [7] and 8 (EN1998-1) [1], under gravity and seismic loading. A four-story, three-bay frame system, designed under a medium ductility class (DCM, behavior factor q = 3.90) and a ground acceleration of $a_{gR} = 0.16 \cdot g$, was considered. Standard gravity loads, and material classes (C20/25 concrete, B500C for steel) were applied. The complete procedure is described in [8].

Fig. 1 depicts the building geometry, highlighting the extracted region from the first story, containing the four selected beam-column joint configurations: a corner joint (A), two identical exterior joints (B, C), and an interior joint (D). All joints are subjected to horizontal (seismic) loading exclusively along the x-x direction. Due to symmetry, the x-x direction for joints A and D is identical to their y-y direction. For joint B, the direction x-x coincides with the direction y-y of joint C, and vice versa. Consequently, all potential joint types and loading directions are considered. The boundary lines separating the four joint configurations are drawn across the midspan of the slabs, while half the column length above and below the joint is considered, approximately corresponding to the point of contraflexure (zero moments), suggesting pinned connection under horizontal loading.

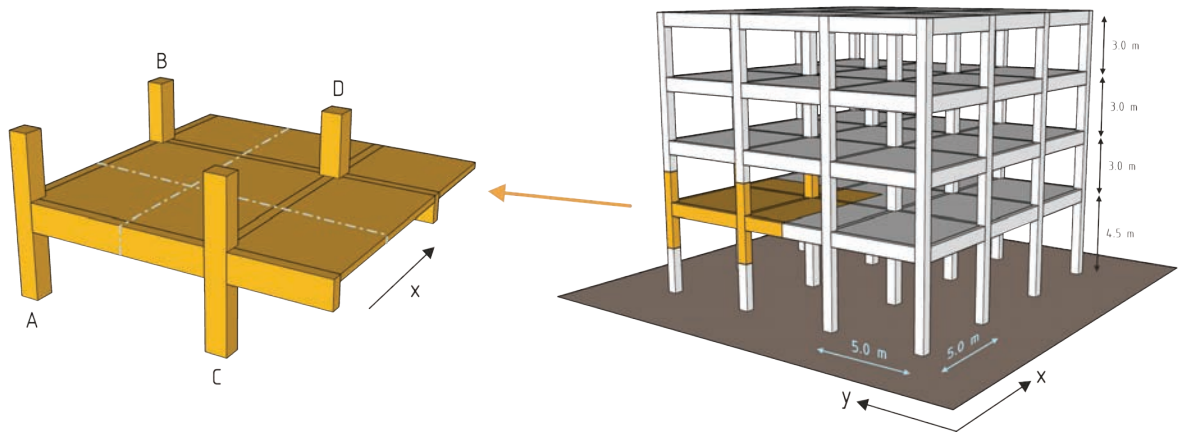

Fig. 1 : Extracting beam-column joint configurations from an R/C frame building.

Table 1 includes the dimensions of the four considered beam-column joints, along with the longitudinal and transverse reinforcement details. It should be noted that under medium ductility class (DCM) [2], the transverse (hoop) reinforcement inside the joint maintains the same spacing as in the critical regions of the adjacent columns. For the slab, the maximum allowable reinforcement spacing of 250 mm was generally applied to establish a lower limit on the possible contribution reinforcement to the slab tensile flange (under negative moment). Without this consideration, it would be a trivial conclusion to attribute any influence of the slab to a possible dense reinforcement spacing (i.e. large reinforcement ratio) at the beam supports.

The R/C - oriented 3D finite element software ATENA [9] was used to model the four selected joint types. Concrete was modeled using eight-node isoparametric solid (brick) elements, with eight integration points and three degrees of freedom per node. To better capture

the inelastic response in the joint and around the beam/column critical regions, a dense mesh of approximately 5 cm (yet larger than the maximum aggregate size) was applied. The non-critical regions were modeled with about double that size to balance the expected computational cost. The slab was modeled in a similar manner, with 4 and 2 elements over its thickness for the dense and coarse regions, respectively. Fixed surface contacts were utilized in an elaborate model assembly procedure, as depicted in Fig. 2.

Properties		Beam-column joint type			
		Corner (A)	Exterior (B)	Exterior (C)	Interior (D)
Column	Dimensions (mm)	450 × 450	500 × 400	400 × 500	500 × 500
	Long. reinf.	8Ø18	4Ø20+4Ø18	4Ø20+4Ø18	8Ø20
	Transv. reinf. (crit. & non crit.)	Ø8/145 Ø8/185	Ø8/145 Ø8/185	Ø8/145 Ø8/185	Ø8/160 Ø8/185
Long. Beam (x-x)	Dimensions (mm)	250 × 650			
	Long. reinf. (top & bot.)	3Ø18+2Ø16 3Ø16+1Ø18	3Ø18+1Ø16 3Ø16	3Ø18 3Ø16	3Ø18+1Ø16 3Ø16
	Transv. reinf. (crit. & non crit.)	Ø8/125 Ø8/165			
Transv. Beam (y-y)	Dimensions (mm)	250 × 650			
	Long. reinf. (top & bot.)	3Ø18+2Ø16 3Ø16+1Ø18	3Ø18 3Ø16	3Ø18+1Ø16 3Ø16	3Ø18+1Ø16 3Ø16
	Transv. reinf. (crit. & non crit.)	Ø8/125 Ø8/165			
Slab	Thickness (mm)	150			
	Reinforcement	Ø8/250			

Table 1: Beam-column joint geometry and reinforcement

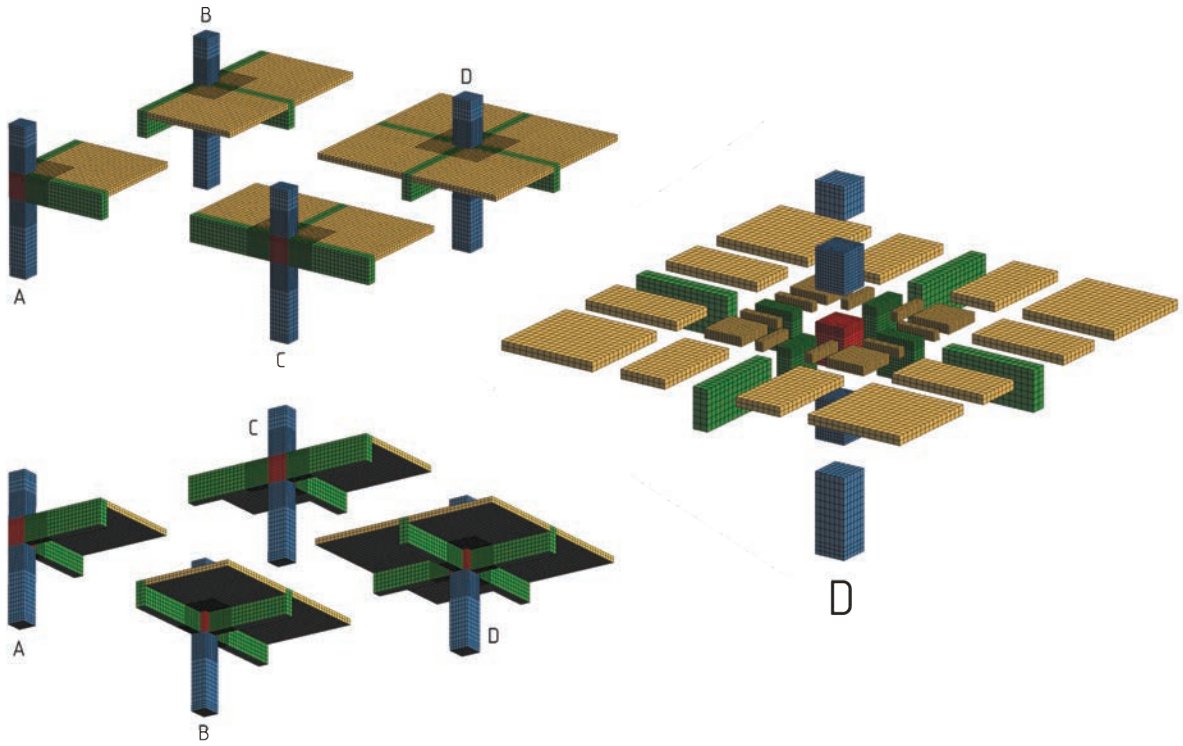

Fig. 2 : Beam-column joint models and coarse/dense region assembly.

Two-node truss elements, with two integration points and one axial degree of freedom per node, were used to model the steel reinforcement bars, which were embedded in the concrete elements. A perfect bond was assumed due to the proper anchoring of all reinforcement bars as per design specifications. Efforts were made to model the reinforcement with a high level of detail, as illustrated in Fig. 3.

In terms of the employed material models, the selected concrete constitutive law (NonLinCementitious2) simulates both tension and compression failure modes. This is achieved through the use of an orthotropic smeared crack formulation and a mesh-independent crack band model for fracture, alongside a Menétrey-Willam based plasticity model for compression. Strains are split into elastic, plastic, and fracturing components, managed by a recursive iterative algorithm. This algorithm can handle dual active failure surfaces and physical changes like crack closure. For reinforcement, a uniaxial multilinear law is employed, allowing for the tracing of all stages of steel behavior, covering both the elastic and inelastic phases. The properties of all materials used in the modeling were calibrated based on Eurocode 2 [1] expressions for the concrete and steel classes (C20/25 and B500C) used in the building.

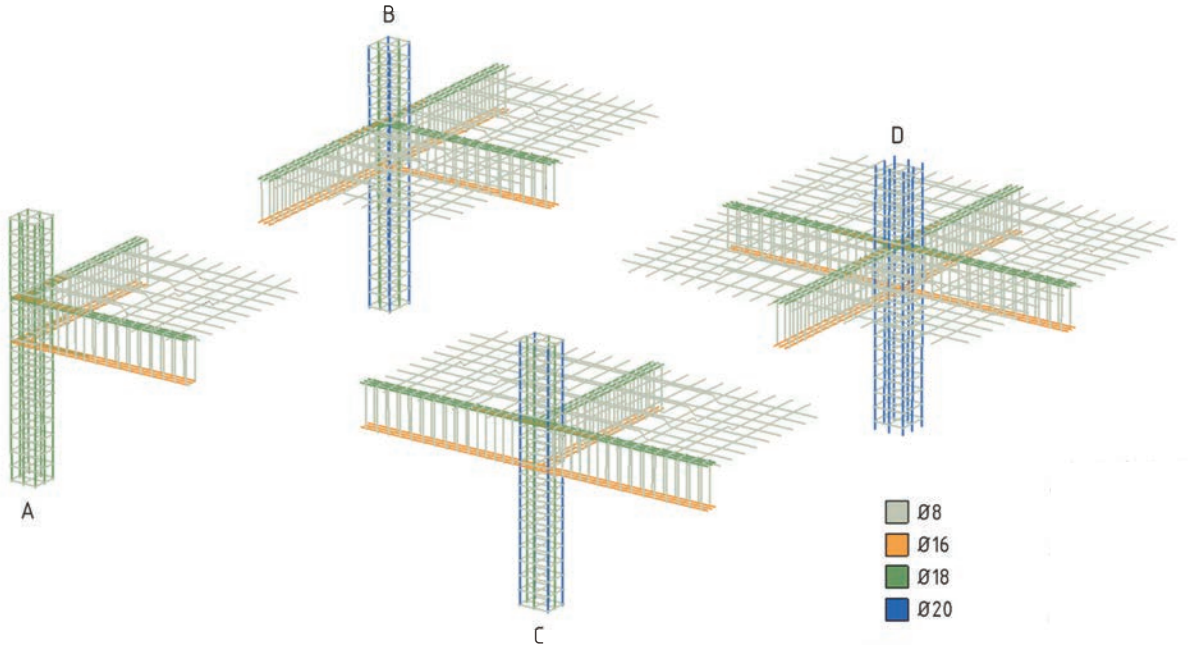

Fig. 3 : Modeling of reinforcement bars.

Loading and boundary conditions were applied in two successive stages, namely gravity and lateral (seismic). The gravity stage included the material self-weight as a volumetric body load (25 kN/m^3) and an axial compression force on the uppermost column section as a surface load. For consistency, the normalized axial force was set to a constant $\nu = 0.2$ in all configurations. The boundary conditions for this stage included (i) vertical support on the bottom column section and (ii) lateral restraints along the beam/slab cut lines in both directions. The lateral loading was applied as a monotonically increasing, prescribed horizontal displacement on the top column section, in small increments, along the x-x direction. The boundary conditions for this stage included (i) a pinned support on the lowermost column section, (ii) lateral restraints for beam/slab cut lines in the y-y direction, and (iii) vertical restraints on the beam/slab cut lines in the x-x direction. The analysis used the modified Newton-Raphson (mNR) iterative scheme with the stiffness matrix updated at each step, appropriate conver-

gence criteria, and a predetermined maximum number of iterations. The expected typical deformed shape for the above loading types was retrieved, as shown in Fig. 4, confirming the integrity of the modeling procedure.

Aligning with the objectives outlined in the introduction section, this study investigates the influence of both the transverse beam and the slab on the inelastic response of beam-column joints. A layered modeling technique was employed, facilitating the efficient compilation of reduced models from the full configurations previously described. This methodology led to the establishment of three distinct modeling levels, depicted in Fig. 5: (i) planar beam-column joints, consisting of a column and a longitudinal beam, (ii) a spatial model including the transverse beam, and (iii) the full model that includes the slab as well. In total, 12 different models are prepared for analysis. The forthcoming numerical results will provide comparative analyses of the three levels based on the inelastic response (pushover) curves, complemented by observations on crack propagation, reinforcement yielding patterns, and failure mechanisms.

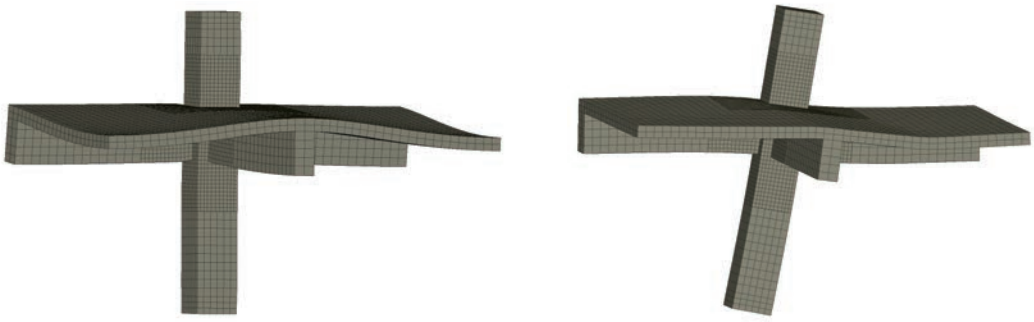

Fig. 4 : Typical deformed shape for gravity (left) and lateral loading (right).

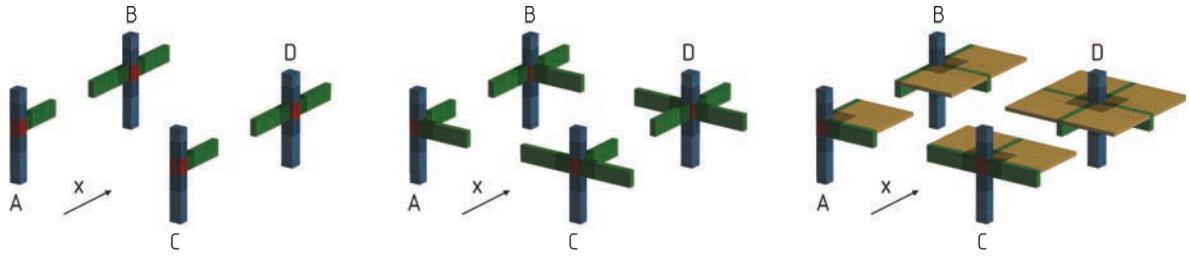

Level 1 : Planar beam-column joint

Level 2 : Addition of transverse beam

Level 3 : Addition of transverse beam and slab (full model)

Fig. 5 : Three modeling levels for comparison purposes.

3 ANALYSIS RESULTS

From the analysis results of the 12 models described in the previous section (see Fig. 5), the global response curves in terms of horizontal displacement (mm) vs. reaction (kN) were drafted and are depicted in Fig. 6 for the four different beam-column joint configurations (A-D). For each configuration, all three modeling levels are superimposed for visual comparison. On the same plots, the maximum and ultimate displacement / reaction are indicated as colored dots. The ultimate displacement / reaction corresponds to the point at which there is an estimated 20 % drop in strength relative to the maximum strength observed. Moreover, the displacement, reaction, and dissipated energy (i.e. area under the capacity curve, in kJ) at the

maximum and ultimate points were quantified in a set of comparative histograms depicted in Fig. 7. For the second and third modeling levels (which include the transverse beam and the slab) the percentile difference with respect to the first level (longitudinal beam only) is indicated.

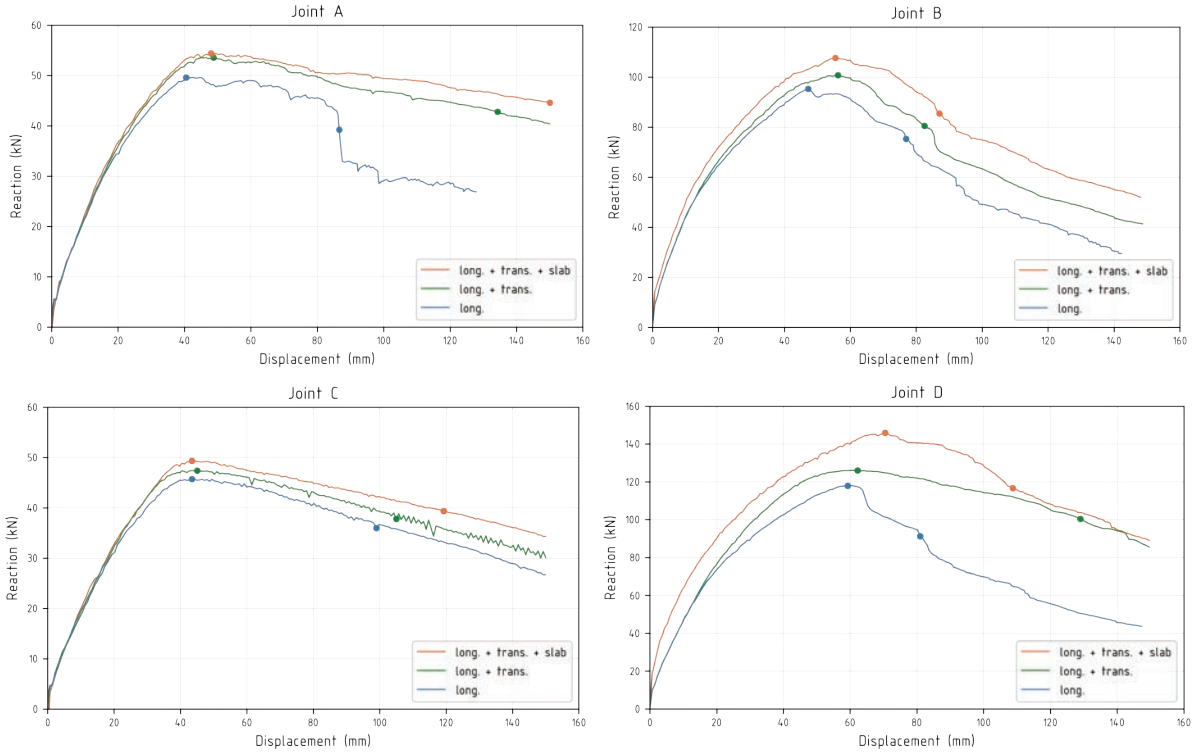

Fig. 6 : Response curves for the four beam-column joint configurations.

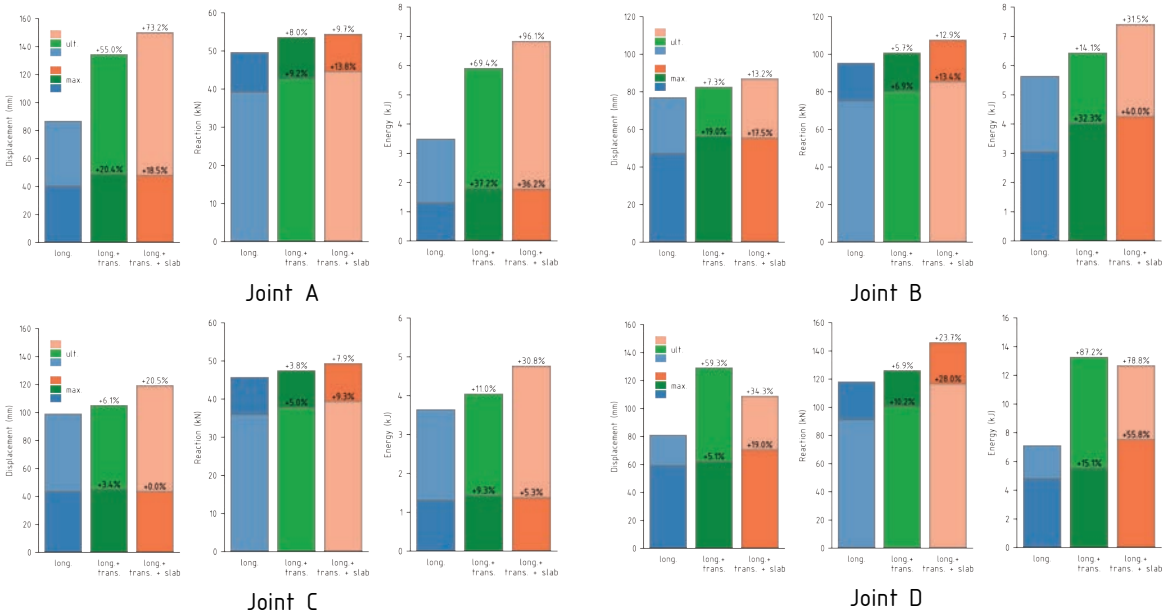

Fig. 7 : Response quantities at maximum and ultimate points for the four beam-column configurations.

It is generally observed that the presence of the transverse beam and the slab enhances both the strength and, notably, the displacement capacity (ductility) of the beam-column joint. Spe-

cifically, when the addition of the transverse beam alone is considered, the maximum strength increases by about 3.8 % to 8.0 %. In the full model that includes the slab, this increase ranges from 7.9 % to 23.7 %. The enhancement for the ultimate displacement varies from 13.2 % up to 73.2 %. The impact of these enhancements becomes even more apparent when the dissipated energy. At the ultimate state, dissipated energy increases from about 31 % for the exterior joints, up to 78.8 % for the interior and 96.1 % for the corner joint. It is deemed that these quantitative results clearly indicate the significant role that the transverse beam and slab play in determining the inelastic response of beam-column joints and, therefore, cannot be easily disregarded when evaluating these joints either experimentally or analytically.

Fig. 8 depicts the cracked state (crack width > 0.3 mm) at the ultimate displacement for the three corner joint models in 3D and 2D views (displaying both vertical faces of the longitudinal beam). Additionally, the stress state of the embedded reinforcement is shown, with solid red and blue colors indicating yielding and compression, respectively.

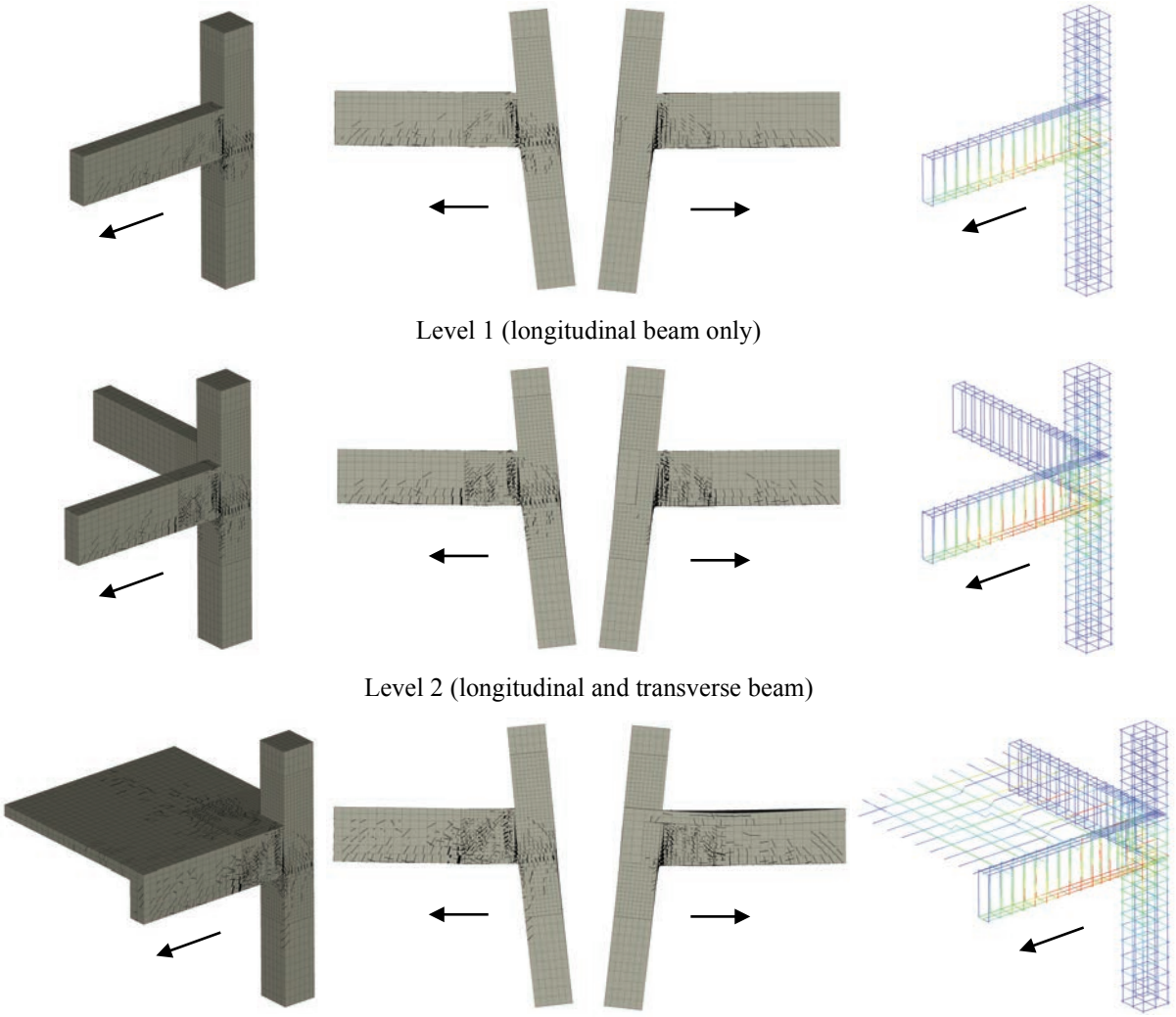

Level 1 (longitudinal beam only)

Level 2 (longitudinal and transverse beam)

Level 3 (longitudinal and transverse beam with slab)

Fig. 8 : Cracked state and reinforcement stress state for corner joint models (arrow indicates loading direction)

For the corner joint (A), flexural cracking is evident at the beam end, and also extends on the outer face of the joint, particularly across its boundary with the underlying column. In contrast, no cracking is observed on its inner face. This may be attributed to the eccentricity

of the longitudinal beam with respect to the column (see Fig. 2). This pattern of damage is further supported by the observable yielding of the transverse (hoop) reinforcement within the joint. The incorporation of the transverse beam (level 2) appears to expedite flexural cracking and reinforcement yielding at the beam end due to its torsional effect on the joint, while the introduction of the slab (level 3) results in beam damage distributed across a longer longitudinal distance. Nonetheless, neither of these additions appears to alleviate the previously observed joint damage.

Fig. 9 illustrates the state of cracking and reinforcement yielding at the ultimate displacement for the two exterior joints – essentially the same joint subjected to two perpendicular loading directions. When the joint is connected to two longitudinal beams along the loading direction (model B), considerable shear cracking is observable on its outer face, together with hoop yielding. Conversely, when the joint only adjoins one longitudinal beam along the loading direction (model C), only flexural cracking at the beam end is apparent, with no discernible damage to the joint itself. The only distinguishing factor between this configuration and the corner joint model (A) is that, in this instance, the beam connects to the joint concentrically. As noted previously, these observations of damage remain consistent across all three model variants (with or without a transverse beam and slab).

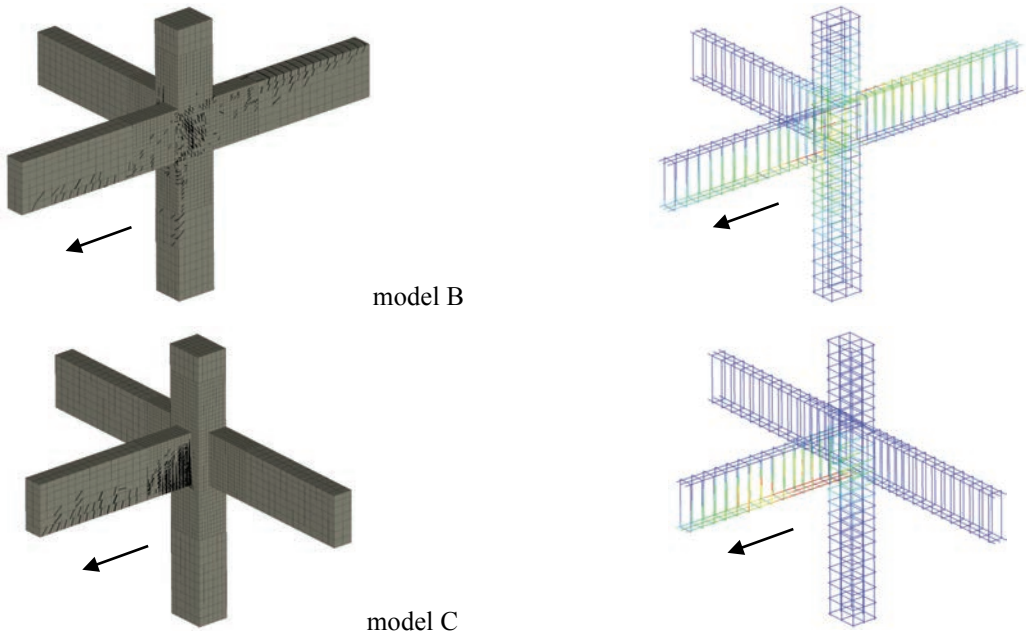

Fig. 9 : Cracked state and reinforcement stress state for exterior joint models (longitudinal and transverse beam).

Fig. 10 illustrates the cracking state at the ultimate displacement in the interior joint (D). In this case, the joint is connected to two longitudinal beams (as in B) and two transverse beams (as in C). Noticeable joint cracking and hoop yielding reappear, and the introduction of transverse beams and the slab does not appear to mitigate any joint damage. Furthermore, Fig. 11 demonstrates the contribution of the slab reinforcement to the (effective) tensile flange of the beam for both the exterior (B) and interior (C) joints, with a more noticeable effect in the latter, as expected. Notably, Eurocode 8 [1] advises accounting for this reinforcement contribution when assessing the beam flexural capacity during capacity design.

These detailed and comprehensive analysis models provide an accurate representation of the behavior and response of beam-column joints, enabling the exploration of additional response effects and phenomena for a more in-depth understanding of their performance. The

models can support future research efforts and inform the development of improved design and evaluation techniques.

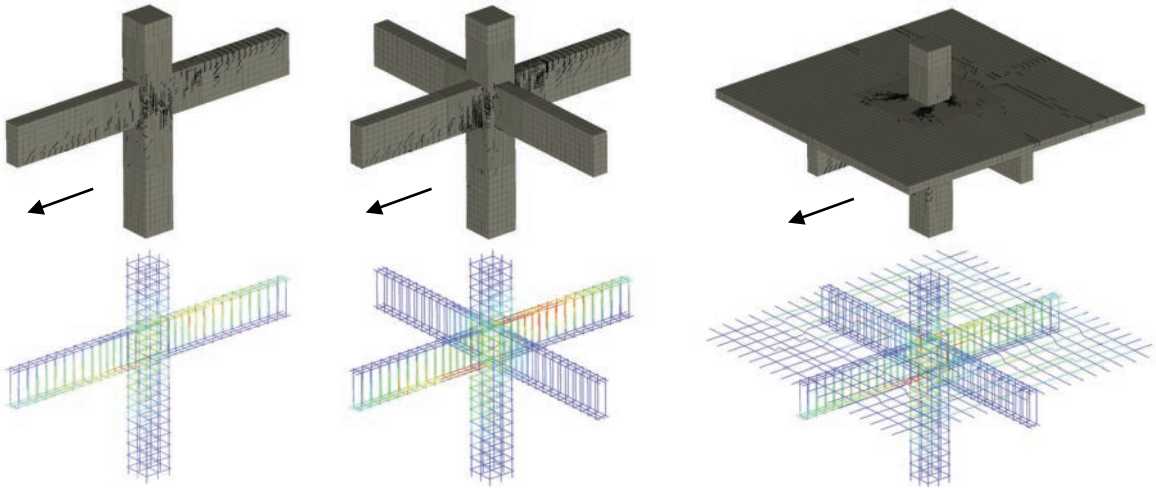

Fig. 10 : Cracked state and reinforcement stress state for the interior joint model (all three variants).

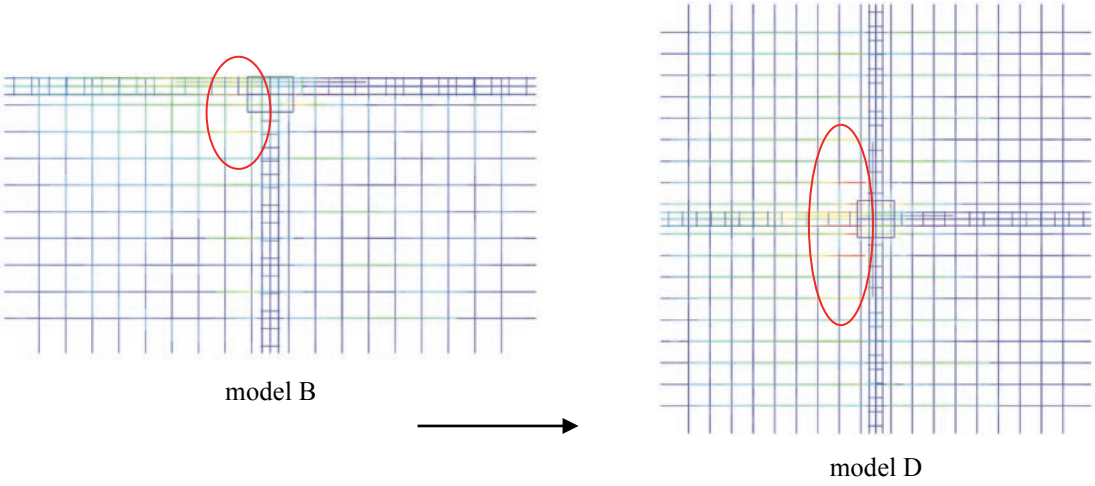

Fig. 11 : Contribution of slab reinforcement to the tensile beam flange for models B (left) and D (right).

4 CONCLUSIONS

The numerical investigation conducted highlights the importance of the transverse beam and the slab in the inelastic response of R/C beam-column joints, a factor often neglected due to cost and implementation constraints in experimental practice. Based on a realistic building setup that adheres to Eurocodes 2 and 8, various joint types were selected and modeled at three distinct levels to allow a thorough examination of this influence.

The presence of the transverse beam and the slab significantly enhances the strength and displacement capacity (ductility) of beam-column joints, suggesting an influential role in directing the joint's inelastic response. The addition of the transverse beam alone results in a noticeable increase in maximum strength. When the slab is included, this enhancement becomes even more substantial. Similarly, the ultimate displacement shows a marked improvement, indicating a notable increase in ductility. This progress means that there is a substantial increase in the dissipated energy at the ultimate state for all joint types. From a qualitative perspective, crack propagation and reinforcement yielding patterns show interesting trends

with the addition of the transverse beam and slab. The transverse beam generally accelerates flexural cracking and reinforcement yielding at the beam end due to its torsional effect on the joint. On the other hand, the introduction of the slab contributes to distributing the beam damage across a longer longitudinal distance. Finally, despite the recommendation in Eurocode 8 to maintain the same hoop spacing in joints as in adjacent columns for medium ductility structures, the detected joint cracking implies an inadequacy of transverse reinforcement. This observation highlights the need for a critical re-evaluation and potential reinforcement enhancement in these areas to improve seismic performance of beam-column joints.

The paper adds to understanding the role of the slab in beam-column joint behavior, particularly in the context of seismic loading. Future studies may include exploring the effect of slab thickness, bond characteristics, reinforcement details, and the influence of bidirectional seismic loads. Furthermore, considering the impact of the slab on joint behavior under different ductility classes could be an interesting topic to investigate. In conclusion, this numerical study presents a robust basis for further exploration and validation through experimental work. Future research will undoubtedly improve knowledge on this complex and critical aspect of reinforced concrete structural behavior under seismic loading.

REFERENCES

[1] CEN Eurocode 8: Design of structures for earthquake resistance, Part 1, EN 1998-1, 2004.

[2] Kam, W. Y., Gallo, P. Q., & Pampanin, S., Influence of slab on the seismic response of sub-standard detailed exterior reinforced concrete beam column joints, 2010.

[3] Allam, S. M., Elbakry, H. M. F., & Arab, I. S. E., Exterior reinforced concrete beam column joint subjected to monotonic loading. Alexandria Engineering Journal, 57(4), 4133–4144, 2018,

[4] Tambusay, A., Suryanto, B., & Suprobo, P., Nonlinear finite element analysis of reinforced concrete beam-column joints under reversed cyclic loading. IOP Conference Series: Materials Science and Engineering, 930(1), 2020.

[5] Santarsiero, G., & Masi, A., Analysis of slab action on the seismic behavior of external RC beam-column joints. Journal of Building Engineering, 32, 2020.

[6] Mou, B., Zhao, F., Qiao, Q., Wang, L., Li, H., He, B., & Hao, Z., Flexural behavior of beam to column joints with or without an overlying concrete slab. Engineering Structures, 199., 2019.

[7] CEN Eurocode 2: Design of concrete structures, Part 1-1, EN 1992-1-1, 2004.

[8] Ignatakis, C., & Sextos, A. Reinforced concrete structures - Detailing according to Eurocodes 2 and 8, in Greek, Open Academic Editions, hdl.handle.net/11419/6413, 2016.

[9] Červenka V., Jendele L., Červenka J. ATENA Program Documentation Part 1 - Theory, Červenka Consulting, Prague, Czech Republic, 2022.